

## INSTABILITY OF WASTE PLUMES ADSORBED ON IRON OXIDE IN SOILS

J. Gruber

Environmental Science Group  
Health, Safety, and Environment Division  
Los Alamos National Laboratory  
Los Alamos, New Mexico 87545

### ABSTRACT

Iron (hydrrous) oxide coatings on the solid matrix dominate adsorption in many soils. Their adsorption characteristics vary considerably with the composition of the soil pore water. If the latter is not sufficiently buffered, the contaminant distribution between solid and soluble soil phases,  $K_d$  ("distribution coefficient"), will change as intruding water differing in chemical composition from the original one in the system progresses through the plume environment. Thus, the  $K_d$ 's at different locations within the plume become time dependent, spatially variable and causally correlated. The conventional constant or stochastic  $K_d$  model is not capable of describing contaminant migration in such a situation.

A geochemical equilibrium model, the so-called triple layer model, has been incorporated into a transport code and is used to calculate the adsorption processes and, thus, the  $K_d$  as a function of environmental parameters. The major processes occurring are: (1) accumulation of a proton reservoir on the surface itself, (2) development of a charge cloud at a distance of several angstroms from the surface, capable of accommodating contaminant ions, and (3) development of a net charge at the oxide/water interface and, consequently, the creation of a cation or anion exchange capacity of the oxide.

Situations are pointed out in which constant/stochastic  $K_d$  models overestimate the degree of geochemical isolation provided by the environment. The migration of a typical medium- or long-lived cationic radionuclide (e.g. Ni63 [half-life, T, 100 yr], Ni59 [T=80,000 yr]) is modeled for a soil environment at pH = 8 containing goethite (a common iron oxide coating) and sodium, calcium, carbonate, and sulfate as typical inorganic pore water constituents. Adsorption processes (1) - (3) in the plume environment are reversed by having water of different chemical composition intrude and change the pore water composition. The major remobilization process is electrostatic destabilization of the surface bonds of protons and contaminant ions.

The contaminant migration velocity and the shape and peak height of the contaminant distribution ("roll front") are considerably different from those obtained for constant  $K_d$  environments. Because at pH = 8, the major portion of the contaminant is adsorbed, the remobilization process is able to increase the soluble concentration of the contaminant several orders of magnitude. In some scenarios, the adsorbed part of the plume is spatially redistributed so that its concentration also increases.

### INTRODUCTION

Contaminant or tracer migration has been observed to not always obey the constant  $K_d$  concept, which assumes a time and spatially invariant solid/solution partitioning of the contaminant,  $K_d$ . One example is the formation of roll front ore deposits (1), another the fast migration of part of the pesticide napropamide in soil (2), a third the front formation in soil columns leached by acid mill tailings solutions (3).

Two approaches have been developed to improve the contaminant transport model: (1) the generalization of the constant  $K_d$  model into the stochastic  $K_d$  model, and (2) the computation of the  $K_d$  from the chemical composition of the soil solution and the solid matrix ("hydrogeochemical transport model").

The first approach still uses the basic assumptions of the constant  $K_d$  model: (a) linearity of the contaminant/soil interactions, i.e. the superposition principle is used to calculate the contaminant concentration in a soil system characterized by a stochastic  $K_d$  spectrum, (b) time invariance of the system, i.e.  $K_d$  does not change with time, and (c) absence of deterministic spatial correlations in the contaminant/soil interactions. These assumptions greatly simplify the solution of the transport equations, thus reducing the costs of modeling.

The second approach to contaminant transport modeling, the computation of the equilibrium solid/solution partitioning, does not need assumptions (a) - (c). Today's understanding of the solid/solution interactions is still in rapid progress and a reliable and sufficiently complete description of real soils is not yet possible. Therefore, hydrogeochemical transport models, although capable of describing a wider variety of effects than the stochastic  $K_d$  models, at present should be used mainly to define problem areas and research needs. For example, they can specify basic environmental situations (scenarios) in which the simpler and less expensive constant/stochastic  $K_d$  model is likely inadequate, or point out threshold values of geochemical and -physical parameters above which the simple  $K_d$  model will fail to describe contaminant migration.

The objective of this paper is the former issue: A hydrogeochemical model has been developed and used to determine under which basic environmental conditions a contaminant roll front might be generated, or in other words, in which situations a water front intruding into a contaminant plume environment will remove adsorbed contaminant from the soil and accumulate it as it moves through the plume much like a snowplow piles up snow as it moves through a street.

Goethite is one of the major adsorbents in soils. Therefore, it will be assumed that the equilibrium

ad- and de-sorption processes in a soil system can be well enough approximated by the ad- and de-sorption processes in a system containing only goethite and water, and no other constituents.

Because the emphasis of this paper is on pointing out some basic situations in which roll fronts may develop, no attempt will be made to quantitatively check the influence of a variation of the physical and chemical system parameters, such as total number of adsorbing sites on goethite and equilibrium constants for adsorption. Also the number of water constituents will be kept small.

#### ADSORPTION MODEL

A geochemical equilibrium model has been incorporated into a transport code to represent the adsorption processes from which the  $K_d$  can be calculated as a function of environmental parameters.

Figure 1, a schematic of the oxide surface, shows the assumed location of the adsorbed ions. The most ab-

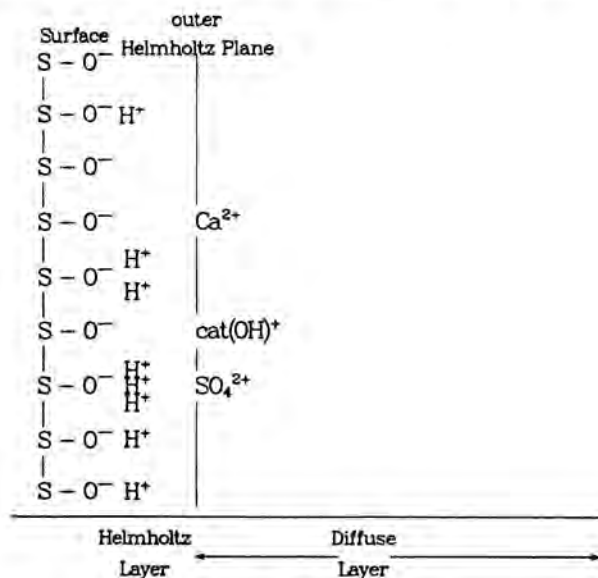


Fig. 1. Schematic representation of adsorbed species.

undant surface species is S-OH, with S denoting the oxide matrix, and OH being a water molecule that has been stripped of one proton. cat is a generic contaminant cation (see Table I for adsorption reaction and surface binding constant).

The mathematical representation of the system is a set of coupled non-linear equations ("triple layer model" (4)), which can be divided into four groups:

- (I) mass action law equations
- (II) Boltzmann equations
- (III) mass and charge balance equations
- (IV) charge/potential relationships.

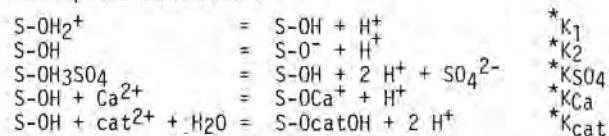
This set of equations represents the coupling between chemical and electrostatic interactions at the solid/solution interface.

TABLE I

Data and Adsorption Reactions used in Computations

Area of Adsorbent ( $F, m^2/l$ ), (1)	300
Capacitance of Helmholtz Layer ( $\mu F/cm^2$ )	110
Capacitance of outer Compact Layer ( $\mu F/cm^2$ )	20
Concentration of Adsorbent ( $S_t, M$ ), (2)	$2.5 \times 10^{-3}$
Total Concentration of Calcium (M), (3)	$10^{-6}$
Total Concentration of Carbonate (M)	$10^{-6}$
Total Concentration of Sulfate (M), Fig. 2	$10^{-6}$
Fig. 3	$10^{-2}$
Total Concentration of Generic Cation (cat, M), (4, 5)	$10^{-8}$
pH, (4)	8.0
Equilibrium Constants for Adsorption Reactions:	
* $K_1$ (M)	$10^{-4.2}$
* $K_2$ (M)	$10^{-10.5}$
* $K_{Ca}$ (-)	$10^{-5.0}$
* $K_{SO4}$ ( $M^2$ )	$10^{-16.7}$
* $K_{cat}$ (M)	$10^{-10.0}$

#### Adsorption Reactions:



#### Equilibrium Constants:

$$\begin{aligned}
 *K_1 &= \frac{[S-OH][H^+]_s}{[S-OH_2^+]}, (5) \\
 *K_2 &= \frac{[S-O^-][H^+]_s}{[S-OH]} \\
 *K_{SO4} &= \frac{[S-OH][H^+]_s^2 [SO_4]_b}{[S-OH_3SO_4]} \\
 *K_{Ca} &= \frac{[S-OCa^+][H^+]_s}{[S-OH][Ca^{2+}]_b} \\
 *K_{cat} &= \frac{[S-OcatOH][H^+]_s^2}{[S-OH][cat^{2+}]_b}
 \end{aligned}$$

#### Comment:

- (1)  $F = p f o (1-n)$   
 where p : fraction of soil particle surface covered by goethite (0.2).  
 f : surface of soil particle per unit weight of particle ( $1 m^2/g$ )  
 o : density of soil particle ( $2.6 g/cm^3$ )  
 n : porosity (0.3)
- (2)  $S_t = F m$   
 where m : number of adsorbing sites per unit area of adsorbent ( $10^{-5} moles/m^2$ )
- (3) total concentration: concentration in the system, consisting of a soluble and an adsorbed part.
- (4) used only in transport calculations (Figs. 4 - 6).
- (5) cat is a generic doubly charged contaminant cation,  $[x]$  is activity of x, which is related to the concentration of x by a correction factor,  $[x]_s$  is activity of x at surface,  $[x]_b$  is activity of x in outer Helmholtz plane.

#### RELEASE OF $H^+$ AND cat UPON CHANGE OF WATER COMPOSITION

Figures 2 and 3 show the pH dependence of the adsorbed proton inventory. In Fig. 2 the total sulfate concentration is negligible ( $10^{-6} M$ ), and in Fig. 3 it is high ( $10^{-2} M$ ). Because the bulk of the adsorbed proton inventory bound in the S-OH complex remains unchanged when environmental parameters are varied, only variations of the inventory about the reference inventory (concentration of adsorbed protons = concentration of adsorbing sites) are plotted. Thus, e.g. the S-O site is considered a proton hole (and counts -1 in the

proton balance), and the  $S-OH_3SO_4$  is counted as +2 protons.

The adsorbed sulfate (see Fig. 3) suppresses the  $S-OH_2$  complex that is present at pH below 7 when no sulfate is adsorbed. It also generates proton holes (dotted curve in Fig. 3), but at pH below 8 the concen-

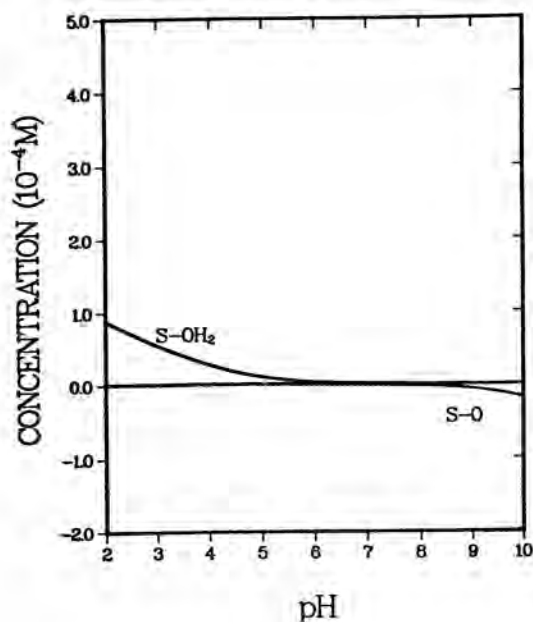


Fig. 2 Surface proton concentration vs. pH for system with total calcium, sulfate and carbonate concentrations equal  $10^{-6}$  M.

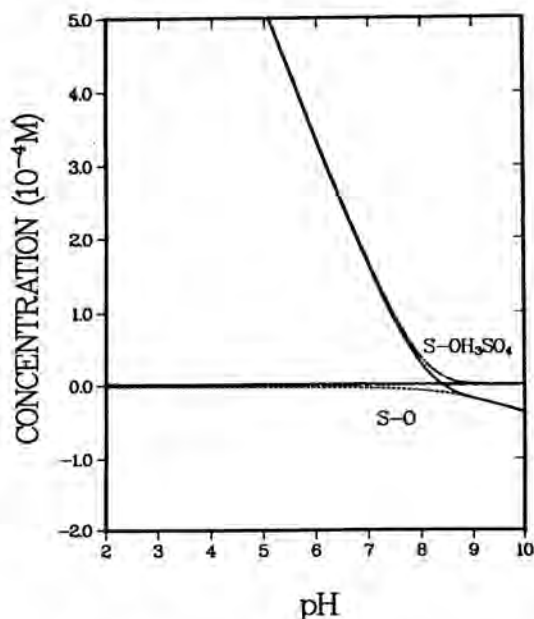


Fig. 3 Surface proton concentration (solid line) vs. pH for calcium, carbonate concentration equal  $10^{-6}$  M and sulfate concentration equal  $10^{-2}$  M. Chain dotted line is the adsorbed sulfate concentration multiplied by 2.

tration of those holes is smaller than the concentration of the protons associated with the  $S-OH_3SO_4$  complex.

Compared to Fig. 2, in Fig. 3 the oxide/water interface is highly charged with protons, because the adsorbing sulfate/proton complex,  $S-OH_3SO_4$ , is strongly bound to the surface. A comparison between Figs. 2 and 3 shows that practically the entire proton inventory of the surface is released, when the high sulfate concentration is reduced to negligible values. In the considered system (Table I) the release is of order  $10^{-5}$  ...  $10^{-4}$  M (equal to 0.01 ... 0.1  $S_t$ ). If these protons are not re-adsorbed into either soluble or adsorbed complexes ("proton buffer"), the free proton concentration in solution will increase. This effect is known as salt titration (5). In our case the pH of the solution would drop to 4 ... 5.

The effect of calcium adsorption on the concentration of surface protons is opposite to the effect of sulfate adsorption because of the opposite charge of the calcium ion: Each adsorbing calcium creates approximately two extra proton holes in the proton "sea" on the surface. If the calcium and sulfate concentrations in water are equal, the concentration of proton holes created by calcium is comparable to the concentration of protons created by sulfate.

At the assumed goethite concentrations (see Table I), sulfate is adsorbed at pH below approximately 7 and calcium above that pH. Therefore the goethite surface releases protons (a) at pH around and below 7 when the sulfate concentration decreases, and (b) at or above pH = 7 when the calcium concentration increases.

A convenient way to characterize adsorption is via the adsorption threshold (also called desorption threshold): It is the pH at which half of the ions are adsorbed, the other half being in solution. Adsorption of cations increases with pH, whereas it decreases for anions with increasing pH. Figure 3 (for pH below 8) is an example of an adsorption curve of an anion near the desorption threshold. For the generic contaminant cation this threshold is around pH = 6 in the simple goethite/water system (no other ions present) at the assumed goethite concentration.

It is evident that in the absence of a sufficient proton buffer the discharge of the adsorbed proton inventory into solution following a variation of the calcium or sulfate concentration has the potential to lower the pH below the adsorption threshold of the generic cationic contaminant. This is the first of two possible contaminant release modes.

Whereas in release mode (1) the pH is lowered below the adsorption threshold, in release mode (2) the threshold is moved to higher pH, which produces a similar release.

An upward shift of the threshold happens when sulfate ions desorb or calcium ions adsorb. The physical reason for the shift is the reduction of the electrostatic contribution to the contaminant adsorption bond.

#### REDISTRIBUTION OF CONTAMINANT PLUMES BY INTRUDING WATER

The combination of release modes (1) and (2) can have a profound effect on the migration of contaminants, because the solid/solution partitioning ratio of the contaminant responds to the pH change (release mode (1)) and the shift of the adsorption threshold (release mode (2)).

In the extreme case the intruding water is able to lower the pH in the entire contaminant plume to a value close to or below the desorption threshold of the contaminant. As a consequence, the inventory of the whole plume gets remobilized and concentrated into a smaller volume. The soluble concentration in the thus formed peak can become considerably larger than the adsorbed concentration in the original plume.

The stronger the pH buffer in the plume or the intruding water, the less the pH drops. The fraction of the adsorbed plume that gets remobilized and spatially concentrated into a peak, and the concentration of the resulting soluble contaminant peak, are much smaller than in case (a) if e.g. the pH does not come as close to the desorption threshold (case (b)).

The reconcentration of (part of) the plume into a high peak of (soluble and/or adsorbed) contamination (which will be called "roll front", henceforth) represents a breach of the "chemical barrier" that would be expected on the basis of the constant Kd model. In addition to that, in the following examples the migration velocity of the peak is several orders of magnitude larger than what the constant Kd model predicts (breach of "retardation barrier").

#### Example 1: Intrusion of Dilute Water into Sulfate Rich Plume Environment

In the first example, a realization of case (a), the release of protons and a cationic contaminant from goethite surfaces and the subsequent accumulation is induced by the intrusion of low sulfate water ( $SO_4^{2-} = 10^{-6}$  M) into a plume environment more concentrated in sulfate ( $10^{-3}$  M). Except for the sulfate concentrations, the compositions of intruding and original plume pore water are identical. All system parameters and concentrations in the plume environment are as given in Table I for Fig. 3.

The plume environment is approximated by an array of cells ("chromatographic column"), through which the water flows from left to right in all following figures. The longitudinal dimension of each cell is chosen so that within each cell complete mixing of the pore water and thermodynamic equilibrium can be assumed.

Figure 4 shows the destabilization of the waste plume with time. The increment between the time steps is the time necessary for the pore water of cell *i* to get into cell *i+1*.

A low pH front develops, which accumulates the protons released upon desorption of sulfate. When the pH has reached a value close to the sulfate desorption threshold, no further sulfate can desorb. Because readsorption or complexation of the released protons is small in this example, the new equilibrium pH lies near the sulfate desorption threshold.

The presence of a buffer, here carbonate is chosen in the intruding water ( $CO_3^{2-} = 10^{-3}$  M), stabilizes the pH in the plume to such an extent that only a minor fraction of the adsorbed contaminant gets reconcentrated (case (b)): The soluble peaks in Fig. 5 are smaller than in the previous scenario (Fig. 4.) Nevertheless, the peak soluble concentration of the contaminant ( $10^{-10}$  M) is roughly two orders of magnitude higher than before the intrusion of the remobilizing water. Because the peak migrates without retardation, both the geochemical and the retardation barriers might still be breached.

#### Example 2: Intrusion of Calcium Rich Water into a Dilute Plume Environment

Figure 6 is another realization of case (a): The pore water in the initial plume environment is dilute in all ions ( $10^{-6}$  M, except for the trace contaminant which is present at  $10^{-8}$  M as in the previous cases). The intruding water is rich in calcium ( $10^{-2}$  M) and carbonate ( $10^{-3}$  M), but otherwise identical to the plume pore water. A calcium concentration of  $10^{-3}$  M together with a carbonate concentration of  $10^{-6}$  M (not shown in a figure) would also lead to a case (a) reconcentration.

When the positive calcium ions adsorb, they release protons from the surface. This, in turn, causes the pH to drop to a value below 6. Since the pH of the intruding water is 8, the pH increases again as the surface proton pool is exhausted. The flatter slope of the pH curve in Fig. 6 (as compared to Fig. 4) is caused by the pH buffer.

## CONCLUSIONS

Repository environments should be investigated with regard to their stability against the mentioned accumulation scenarios.

Large concentrations ( $10^{-2}$  ...  $10^{-3}$  M) of strongly adsorbing electrolytes in either the contaminant plume or the potentially intruding water lead to large proton or proton hole concentrations and electrostatic forces on the oxide surface. Roll fronts of soluble or adsorbed contaminant might form, breaching the initially present geochemical and retardation barriers. To be stable against such a scenario, the plume environment should contain a proton buffer capable of damping the possible proton fluctuations originating from instabilities of the surface proton pools on the oxide.

Strong variations of the point of zero charge with solution composition are indicative of unstable large surface proton pools and of electrostatic force fluctuations. Goethite is an example of an oxide with such an instability. Soils containing those oxides are likely to need efficient proton buffers in order to be sufficiently resistant against contaminant roll front generation.

## ACKNOWLEDGEMENT

This research was sponsored by the University of California at Riverside "Toxic Substances Research and Training Program", at Los Alamos National Laboratory in collaboration with the LANL Environmental Science Group.

## REFERENCES

1. H. C. Granger and C. G. Warren, "Unstable Sulfur Compounds and the Origin of Roll-Type Uranium Deposits," *Economic Geology* 64, 160-171 (1969).
2. W. A. Jury, H. Elabd and M. Resketo, "Field Study of Napropamid Movement through Unsaturated Soil," *Water Resources Research* 22, 749-755 (1986).
3. S. R. Peterson, et al., "Predictive Geochemical Modeling of Interactions between Uranium Mill Tailings Solutions and Sediments in a Flow-Through System," NUREG/CR-3404 (PNL-4782) (1983).
4. J. A. Davis et al., "Surface Ionization and Complexation at the Oxide/Water Interface," *Journal of the Colloid and Interface Science* 63, 480-499 (1978) and 74, 32-42 (1980).
5. J. A. Davis, "Adsorption of Trace Metals and Complexing Ligands at the Oxide/Water Interface," Ph.D. Thesis, Department of Civil Engineering, Stanford University, Stanford, CA 94305 (1977).

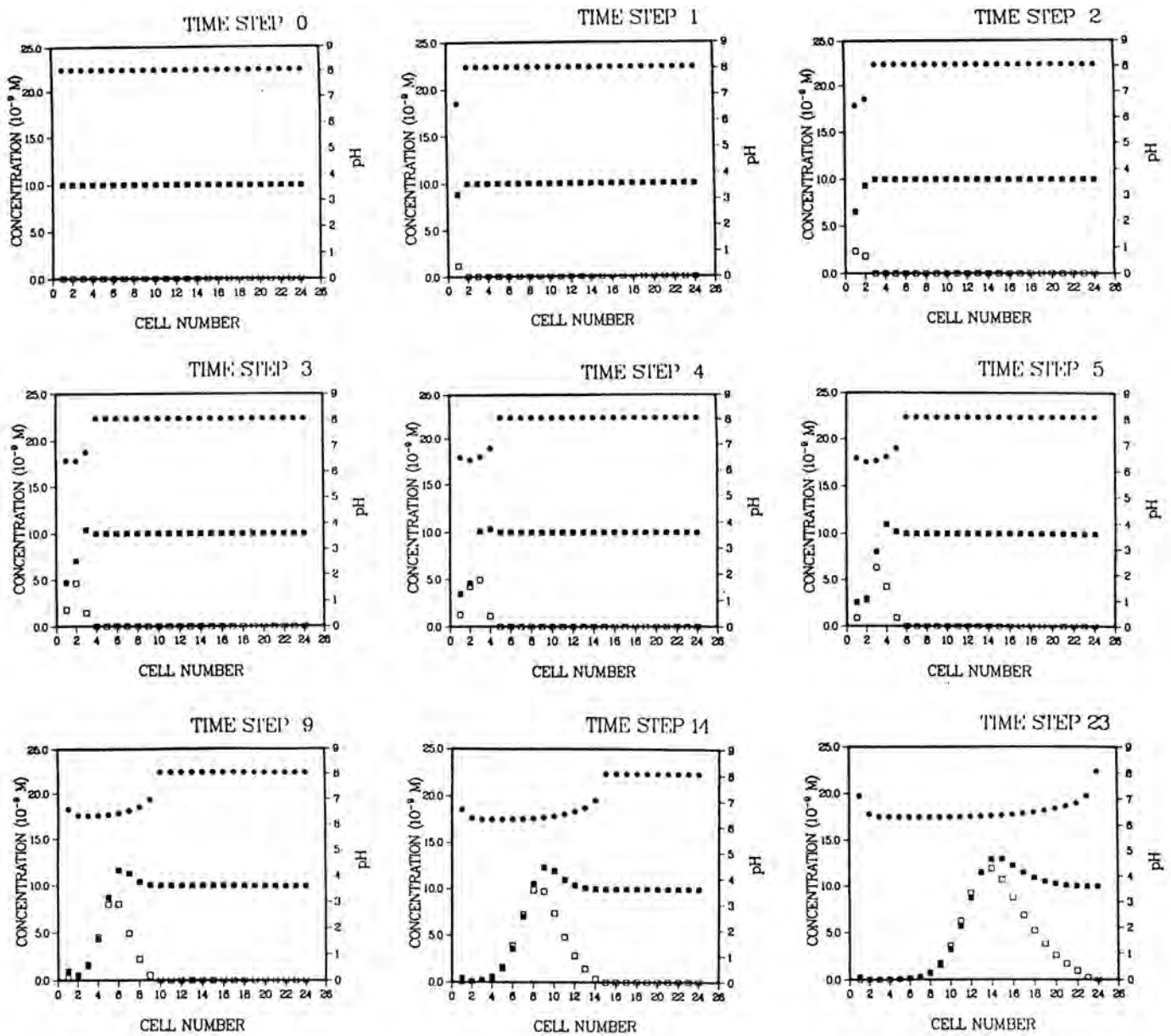


Fig. 4. Development of pH and contaminant fronts in a plume environment originally characterized by pH = 8, calcium and carbonate concentration =  $10^{-6}$  M, and sulfate concentration =  $10^{-2}$  M. The intruding water is identical to the one in the original plume environment, except for a lower sulfate concentration ( $10^{-6}$  M). Closed circles: pH, closed (open) squares: adsorbed (soluble) contaminant.

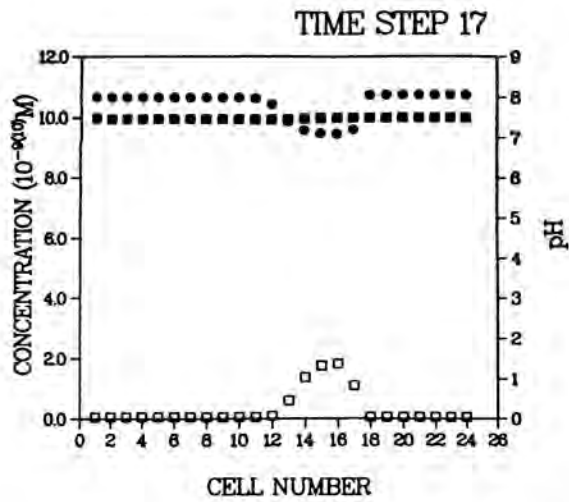


Fig. 5. Front generation in a buffered environment ( $\text{CO}_2^t = 10^{-3}$  M in intruding water, all other concentrations are as given in Fig. 4)

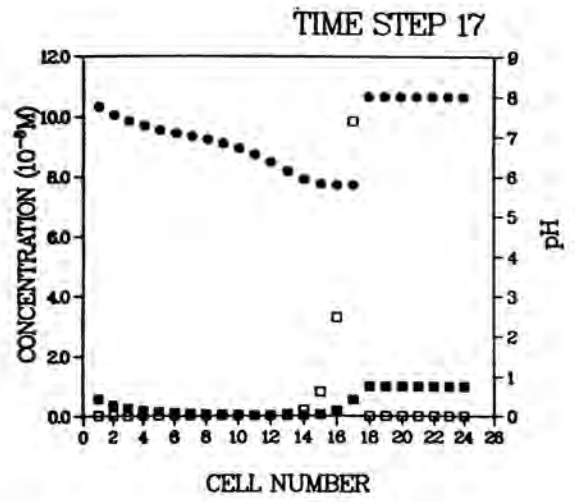


Fig. 6. Front generation in a buffered environment. The protons are released from the surface by intruding calcium rich water ( $\text{Ca}_t = 10^{-2}$  M). Except for the buffer concentration ( $10^{-3}$  M in the intruding water), all other concentrations are  $10^{-6}$  M.